



Thoracic positron emission tomography: ^{18}F -fluorodeoxyglucose and beyond

Timothy J. Jaykel, Michael S. Clark, Daniel A. Adamo, Brain T. Welch, Scott M. Thompson, Jason R. Young, Eric C. Ehman

Department of Radiology, Mayo Clinic, Rochester, Minnesota, USA

Contributions: (I) Conception and design: All authors; (II) Administrative support: TJ Jaykel, EC Ehman; (III) Provision of study materials or patients: All authors; (IV) Collection and assembly of data: All authors; (V) Data analysis and interpretation: None; (VI) Manuscript writing: All authors; (VII) Final approval of manuscript: All authors.

Correspondence to: Timothy J. Jaykel, MD. Department of Radiology, Mayo Clinic, 200 First Street SW, Rochester, MN 55905, USA.

Email: Jaykel.Timothy@mayo.edu.

Abstract: Ongoing technologic and therapeutic advancements in medicine are now testing the limits of conventional anatomic imaging techniques. The ability to image physiology, rather than simply anatomy, is critical in the management of multiple disease processes, especially in oncology. Nuclear medicine has assumed a leading role in detecting, diagnosing, staging and assessing treatment response of various pathologic entities, and appears well positioned to do so into the future. When combined with computed tomography (CT) or magnetic resonance imaging (MRI), positron emission tomography (PET) has become the *sine quo non* technique of evaluating most solid tumors especially in the thorax. PET/CT serves as a key imaging modality in the initial evaluation of pulmonary nodules, often obviating the need for more invasive testing. PET/CT is essential to staging and restaging in bronchogenic carcinoma and offers key physiologic information with regard to treatment response. A more recent development, PET/MRI, shows promise in several specific lung cancer applications as well. Additional recent advancements in the field have allowed PET to expand beyond imaging with ^{18}F -fluorodeoxyglucose (FDG) alone, now with the ability to specifically image certain types of cell surface receptors. In the thorax this predominantly includes ^{68}Ga -DOTATATE which targets the somatostatin receptors abundantly expressed in neuroendocrine tumors, including bronchial carcinoid. This receptor targeted imaging technique permits targeting these tumors with therapeutic analogues such as ^{177}Lu labeled DOTATATE. Overall, the proper utilization of PET in the thorax has the ability to directly impact and improve patient care.

Keywords: Positron emission tomography (PET); positron emission tomography/computed tomography (PET/CT); positron emission tomography/magnetic resonance imaging (PET/MRI); pulmonary nodule; bronchogenic carcinoma

Submitted Apr 23, 2020. Accepted for publication May 26, 2020.

doi: 10.21037/jtd-2019-cptn-09

View this article at: <http://dx.doi.org/10.21037/jtd-2019-cptn-09>

Introduction

Since the early 2000's, there have been many advancements in nuclear medicine which have become applicable to diagnosis and treatment of thoracic disorders. The most established application is positron emission tomography (PET). There is a broad base of evidence supporting the

use of ^{18}F -fluorodeoxyglucose (FDG) PET combined with computed tomography (CT) (PET/CT) for evaluation of solitary pulmonary nodules and in the staging and follow up in patients with bronchogenic carcinoma. More recently, hybrid PET/MRI has shown promise in applications within these same diseases. At the same time, there has been development of novel radiotracers, chiefly those which

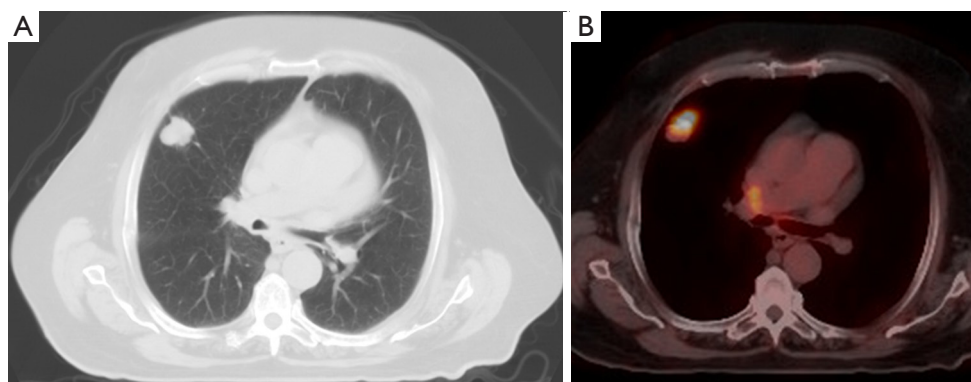


Figure 1 A 74-year-old man found to have a pulmonary nodule at chest radiograph (not shown). Axial CT image (A) shows a nodule in the right upper lobe with indistinct margins. Fused axial images from ^{18}F -FDG PET/CT (B) show marked FDG uptake within this lesion, highly suspicious for carcinoma. The lesion ultimately underwent biopsy, confirming lung adenocarcinoma.

target the somatostatin receptor, most commonly ^{68}Ga -DOTATATE, which have revolutionized not only the imaging diagnosis in patients with neuroendocrine tumors such as bronchial carcinoid, but offer novel therapeutic options via targeted molecular therapies such as ^{177}Lu -DOTATATE. The goal of this article is to provide an overview of current and emerging PET applications in thoracic neoplasms.

^{18}F -FDG PET/CT

^{18}F -FDG is a glucose analog that once taken up within a cell, is trapped within the cell and used as a surrogate marker for glucose metabolism. Glucose metabolism can be seen in a wide variety of situations including normal physiology, but can be increased in pathologic states such as infection or neoplasm. Initially developed in the early 2000's, FDG PET/CT exam volumes have increased considerably over time, and these studies now comprise a cornerstone of oncologic imaging. Oncologic applications of ^{18}F -FDG PET/CT include the evaluation of pulmonary nodules and the diagnosis and staging of bronchogenic carcinoma.

Pulmonary nodules

Pulmonary nodules are a frequent incidental finding when imaging the chest. Older literature estimates that there are 150,000 new pulmonary nodules detected per year in the United States, although this number has likely increased given increased usage of CT (1). The first

approved indication for ^{18}F -FDG PET/CT was for the characterization of solitary pulmonary nodules (2-5). A solitary pulmonary nodule (SPN) is defined as a round, solid, non-calcified lung lesion measuring <30 mm in mean diameter (6). Pulmonary nodules can be characterized as either solid or subsolid.

Solid pulmonary nodule

One of the most important factors for the evaluation of pulmonary nodules with ^{18}F -FDG PET/CT is size. The spatial resolution of PET limits the evaluation pulmonary nodules less than 10 mm with older technology, such as a two-dimensional (2D) acquisition. Under this size, SUV can underestimate the true nodule metabolism, decreasing the negative predictive value (NPV). Advancements in PET imaging such as newer 3D and time-of-flight (TOF) acquisitions are now routine at most institutions; improving the NPV of small nodules and helping the characterization of nodules as small as 7–8 mm (7,8).

The definition of an ^{18}F -FDG PET positive solid pulmonary nodule has changed throughout the years. The previously described SUV max “cut off” of 2.5 is no longer recommended (9). It is now recommended to correlate to internal controls with a SUV max less than blood pool being very likely benign. The accuracy of ^{18}F -FDG PET/CT has proven to be to quite exceptional. In a recent meta-analysis reviewing 44 studies and over 2,800 nodules, the sensitivity was 95%, specificity 82%, PPV 91%, and NPV 90% (10). An example of FDG PET/CT used in the evaluation of a solitary pulmonary nodule is shown in *Figure 1*.

False positives for FDG avid SPN mainly include

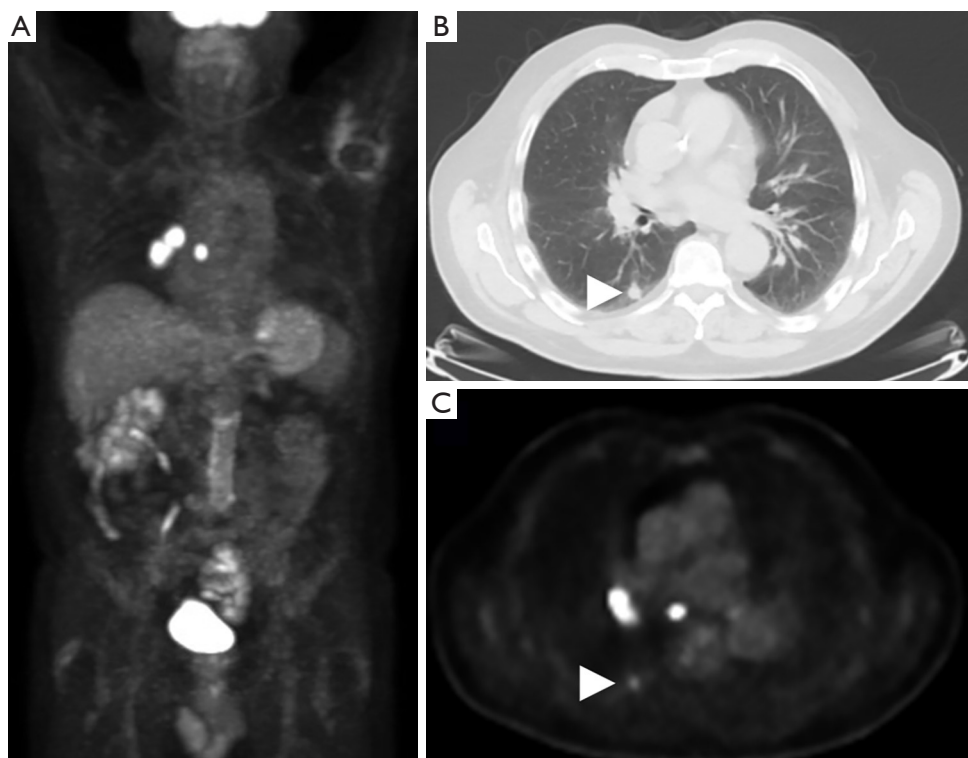


Figure 2 A 78-year-old female with a right lower lobe pulmonary nodule, incidentally seen on CT to assess aortic dissection repair, was further characterized with FDG PET/CT (A). Axial CT (B) and PET (C) images demonstrate a mildly FDG avid right lower lobe pulmonary nodule (arrowheads, SUVmax 2.2) and markedly FDG avid right hilar lymphadenopathy (SUVmax 13.6). Discordant degree of uptake within the nodule versus the draining lymphadenopathy is most consistent with an infectious etiology, specifically chronic fungal infection (so called “flip-flop-fungus” sign). Serological evaluation was positive for histoplasmosis.

granulomatous processes (11). These can be broken down into infectious or inflammatory etiologies. Infectious diseases include bacterial, mycobacterial, and fungal diseases. The prototypical infection is histoplasmosis. Helpful discriminatory factors can include the so called Flip-Flop Fungus sign (*Figure 2*). In fungal infections, the FDG avidity of the SPN is less than the mediastinal/hilar lymphadenopathy. The opposite is true in malignancy, where the FDG avidity of the SPN is typically greater than the FDG avidity of the mediastinal/hilar lymphadenopathy (12).

Inflammatory processes that can have FDG avid SPNs include sarcoidosis, granulomatosis with polyangiitis, organizing pneumonia (*Figure 3*), or rheumatoid nodules. Helpful discriminatory factors are non-specific, but can include fluctuations in growth or a waxing and waning nature over time (13).

False negatives of SPN are also possible. This occurs in the setting of a malignancy that does not have increased

glucose metabolism. The most well-known example is of carcinoid tumor, with a false negative rate of 85% (14). Consideration of alternative diagnoses and further evaluation with other tests such as ^{68}Ga DOTATATE which will be described later should be considered in order to avoid false negative diagnoses. Additionally, metastatic disease from mucinous origins also generally have lower FDG uptake (15).

Subsolid pulmonary nodules

A pulmonary nodule that is not homogenous soft tissue attenuation is referred to as a subsolid pulmonary nodule. Subsolid pulmonary nodules pose many challenges for PET imaging associated with technical factors of image acquisition which can result in a perceived or quantitative decrease in FDG uptake (16). While a subsolid pulmonary nodule may be the manifestation of infectious or inflammatory etiologies, minimal and noninvasive adenocarcinoma lesions may also have this appearance.

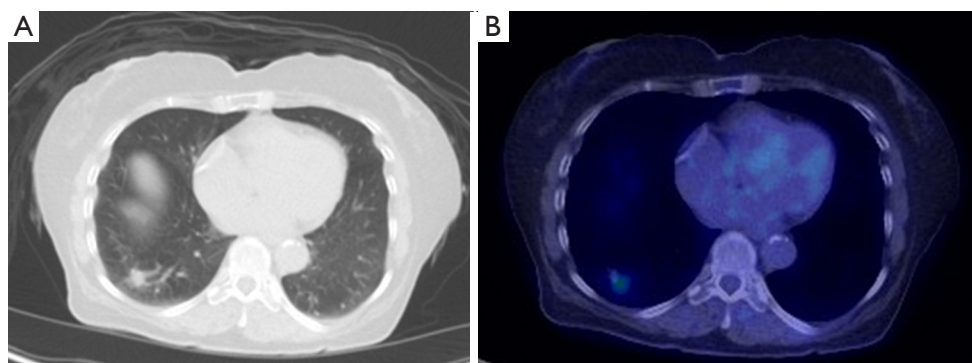


Figure 3 A 69-year-old man with a previous metastatic malignancy with enlarging right lower lobe pulmonary nodule (A). Fused axial images from ^{18}F -FDG PET/CT (B) demonstrate minimal FDG uptake. The pulmonary nodule was biopsied and was negative for malignancy but was consistent for focal organizing pneumonia.

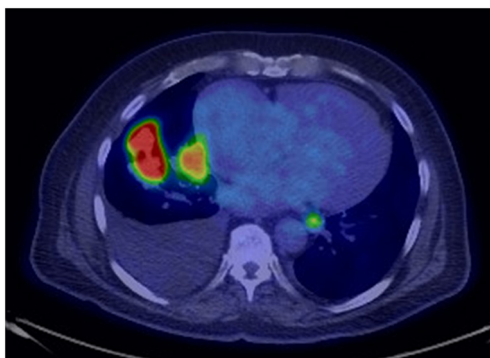


Figure 4 A 68-year-old man with metastatic squamous cell carcinoma presents for restaging. Axial fused ^{18}F -FDG PET/CT demonstrates an FDG avid right middle lobe primary tumor and a large left pleural effusion without uptake. Laboratory testing of the thoracentesis was negative for malignancy.

Subsolid pulmonary nodules can be further classified as pure ground glass nodule or a part solid nodule. A pure ground glass nodule is defined as hazy increased attenuation in the lung that does not obliterate the bronchial or vascular margins. A part solid nodule consists of both pure ground glass and solid soft tissue attenuation (6). The utility of PET/CT in subsolid nodules was investigated by Chun *et al.* in 2008. This study demonstrated perhaps counterintuitively that in part solid nodules, the SUVmax was significantly higher in inflammatory lesions compared to malignant tumors. A threshold-value SUVmax of 1.2 predicted malignancy with sensitivity, specificity, accuracy, PPV and NPV of 62.1%, 80.0%, 70.4%, 78.3% and 64.5%, respectively. Furthermore, above an SUV max of

2.6, all lesions were inflammatory. For pure ground glass nodules, there was no statistical differences in SUV max between inflammation and malignancy (17). Ultimately, differentiation between infectious/inflammatory subsolid nodules and adenocarcinoma spectrum lesions remains challenging and may serve as a future area of investigation.

Bronchogenic carcinoma

Bronchogenic carcinomas are traditionally characterized as either non-small cell lung cancer (NSCLC) or small cell lung cancer (SCLC). While all types of bronchogenic carcinoma are typically FDG avid (*Figures 4,5*), malignancies along the adenocarcinoma spectrum can be variable in their uptake.

Lung adenocarcinoma can have multiple imaging appearances including solid, pure ground glass, and part solid nodules. The solid type usually presents as a SPN where ^{18}F -FDG PET/CT can be helpful as previously described. In the case of ground glass nodules, PET/CT is usually not as helpful in primary lesion characterization. FDG avid ground glass nodules are often infectious or inflammatory, but non FDG avid ground glass nodules could still represent adenocarcinoma. In the case of part solid lesions, PET/CT may have utility for the detection of FDG uptake in the solid component.

The utility of ^{18}F -FDG PET/CT in bronchogenic carcinoma can be separated into staging, prognosis, and post treatment imaging.

NSCLC staging

NSCLC staging with ^{18}F -FDG PET/CT is a widely supported practice, endorsed by multiple organizations

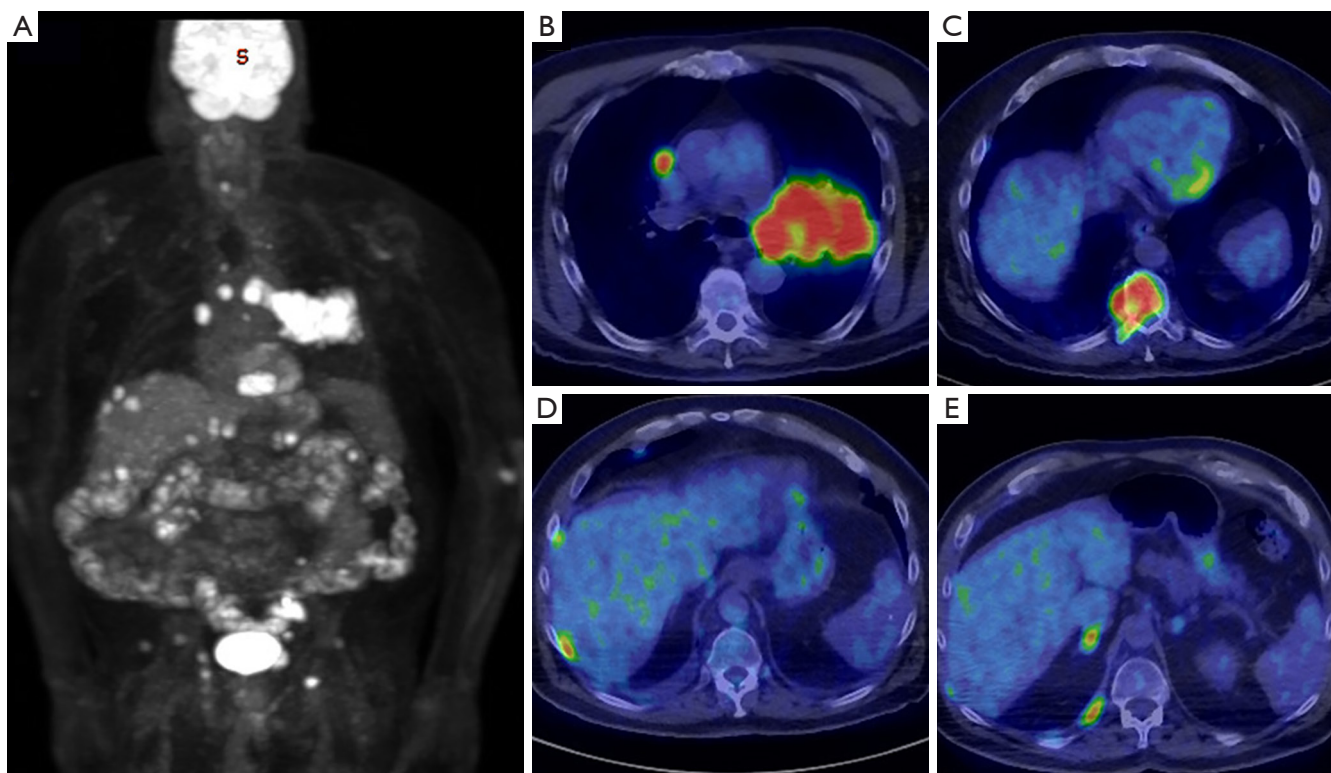


Figure 5 A 74-year-old male presenting with shortness of breath and fatigue. MIP reconstruction from FDG PET (A) shows a large FDG avid left small cell lung cancer with numerous additional foci of abnormal uptake throughout the body. Fused axial PET/CT images reveal that bilateral hilar lymph nodes (B), vertebral body (C), liver (D), and the adrenals (E) have metastatic disease.

including the National Comprehensive Cancer Network (NCCN), the American College of Radiology Appropriateness Criteria, the Society of Nuclear Medicine and Molecular Imaging, and the American College of Chest Physicians (18-20). NSCLC staging is based on the TNM staging criteria. Overall, the addition of PET/CT in lung cancer staging can affect the final lung cancer stage, with studies showing the addition of PET/CT may lead to upstaging in 6.4–41.1% of patients and downstaging in 9.5–12.3% of patients (21,22).

NSCLC T staging

Lung cancer T staging describes the tumor size and invasive features and is separated into four categories, T1–T4 (23). Specific PET imaging characteristics are listed for each (Table 1).

NSCLC N staging

The N staging is used to classify lymph node involvement and is separated into three categories N1–N3. N1 nodes

include ipsilateral intrapulmonary, peribronchial, and hilar lymph nodes. N2 nodes include ipsilateral mediastinal or subcarinal lymph nodes. N3 nodes include contralateral hilar or mediastinal lymph nodes, ipsilateral or contralateral scalene nodes, and supraclavicular lymph nodes. A positive lymph node is defined as a SUV max greater than the SUV max of the mediastinal blood pool.

Lung cancer N staging is where the utility of PET/CT has excelled due to limitations of conventional CT imaging. While conventional imaging can accurately demonstrate lymph node size, PET/CT can also image metabolic differences within a lymph node (Figure 6). In a study by Gould *et al.* in 2003, nodal metastases detection by conventional CT had sensitivity of 61% and specificity of 79%. With PET/CT, this was improved to a sensitivity of 85% and a specificity of 90% (24). These results were later confirmed in a 2013 meta-analysis of 56 studies with pooled FDG PET/CT sensitivities and specificities of 72% and 91% respectively in determining mediastinal nodal staging. The value of this improved detection has a direct

Table 1 T category, based on size and degree of invasion

T category	Size	Invasion	PET utility
T1	0 to ≤3 cm	Minimally invasive	FDG PET/CT may be of limited benefit for detecting these smaller lesions below 7–8 mm, especially if the lesion is subsolid
T2	>3 to ≤5 cm	Invasion of the main bronchus, visceral pleura, atelectasis, or obstructive pneumonitis	FDG PET/CT may play an important role in this category, as it is superior to conventional CT in differentiating between tumor and post obstructive atelectasis; while atelectasis is more FDG avid than normal aerated lung, atelectasis is less FDG avid than tumor
T3	>5 to ≤7 cm	Invasion of the chest wall, phrenic nerve, and parietal pericardium; a tumor nodule in the same lobe as the primary tumor	FDG PET/CT may be beneficial in detecting additional pulmonary nodules; one important consideration, in this category is that FDG PET/CT is suboptimal to assess chest wall invasion due to blooming artifact, which may overestimate chest wall invasion; however, PET/MRI may be useful
T4	>7 cm	Invasion of the diaphragm, mediastinum, carina, trachea, heart, great vessels, recurrent laryngeal nerve, esophagus, or vertebral body; T4 disease also includes a tumor nodule in a different ipsilateral lobe	FDG PET/CT may be helpful in detecting the additional nodules in a different ipsilateral lobe; an indirect finding that implies recurrent laryngeal nerve involvement includes increased FDG uptake in the contralateral vocal cord, due to compensatory increased activity of that cord

PET utility depends on T category.

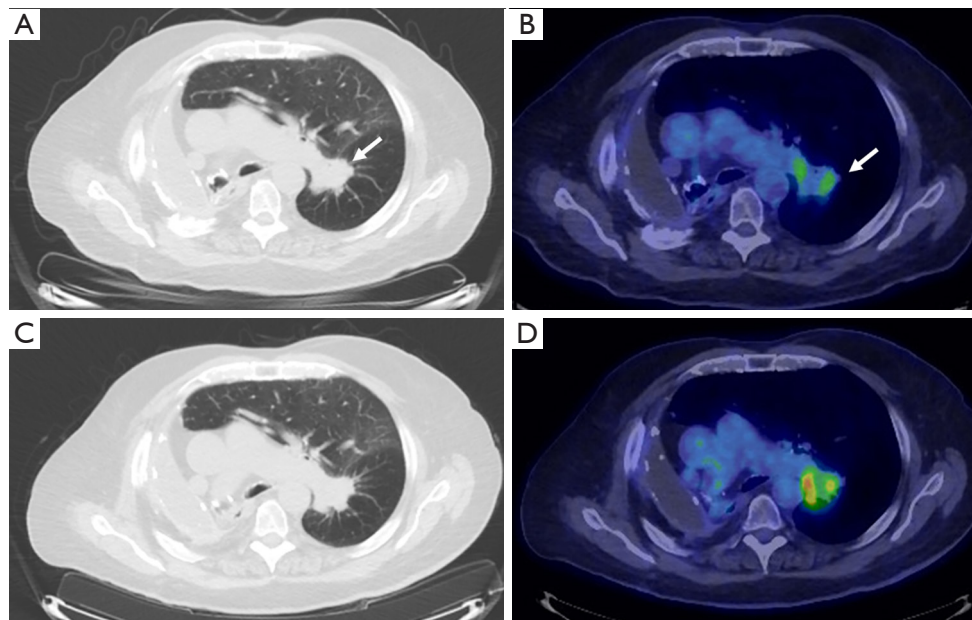


Figure 6 A 74-year-old man status post right pneumonectomy for squamous cell carcinoma was imaged for surveillance. Axial CT (A) and fused FDG PET/CT (B) images show mild uptake in the left hilum (arrows). Follow-up scan obtained 4 months later demonstrated unchanged size (C) but interval increase FDG uptake in the hilar mass (D), suspicious for recurrent disease.

Table 2 M category by location

M category	Involvement	PET utility
M1a	Tumor nodule in contralateral lung; tumor with pleural or pericardial nodules or malignant pleural or pericardial effusion	Features of a malignant effusion include diffuse uptake above blood pool or rim increased FDG uptake
M1b	Solitary single-organ extrathoracic metastasis	Whole body imaging
M1c	Multiple extrathoracic metastases in one or multiple organs	Whole body imaging

PET is particularly useful in the evaluation of distant metastases.

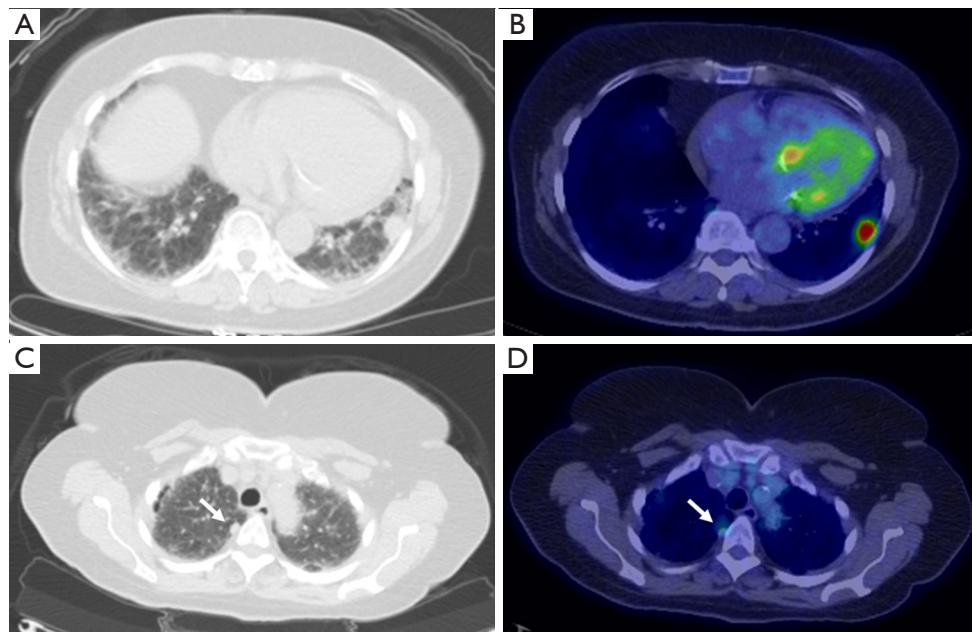


Figure 7 A 74-year-old woman with biopsy proven left lower lobe bronchogenic carcinoma. Index lesion is shown on axial CT image (A) with increased FDG uptake (B). Smaller right upper lobe pulmonary nodule (arrows) on axial CT (C) also demonstrates mild increased FDG uptake (D). This nodule was biopsied and confirmed to represent metastatic deposit.

impact on patient care. In the findings of a prospective multicenter trial in 2015, management strategies changed in approximately 72% of cases of lung cancer when FDG PET/CT examinations were used (25).

NSCLC M staging

Utility of FDG-PET in lung cancer M staging is shown in *Table 2*. PET/CT is excellent for detecting distant metastases, including metastases in the contralateral lung (*Figure 7*). In a recent meta-analysis, the sensitivity, and specificity of ^{18}F FDG PET/CT for all distant metastasis was 93% and 96% respectively (26). Bone metastases were detected with a sensitivity of 90% and specificity of 98% (27). PET/CT is very helpful for adrenal metastases with a

sensitivity of 93% and specificity of 90% (28). PET/CT is also excellent for liver metastases, however, this is less well studied. The major weakness of PET/CT in the setting of M disease is for the evaluation of brain metastases due to the high background normal brain activity (24). However, brain metastases can occasionally be detected (*Figure 8*), appearing as either as relatively hypermetabolic or hypometabolic foci.

False positive

While the diagnostic accuracy of PET is quite good, reaching up to 93.5%, this still leaves a 6.5% false positive rate (29). The most common causes of false positives are due to inflammatory pseudotumor and tuberculosis. False

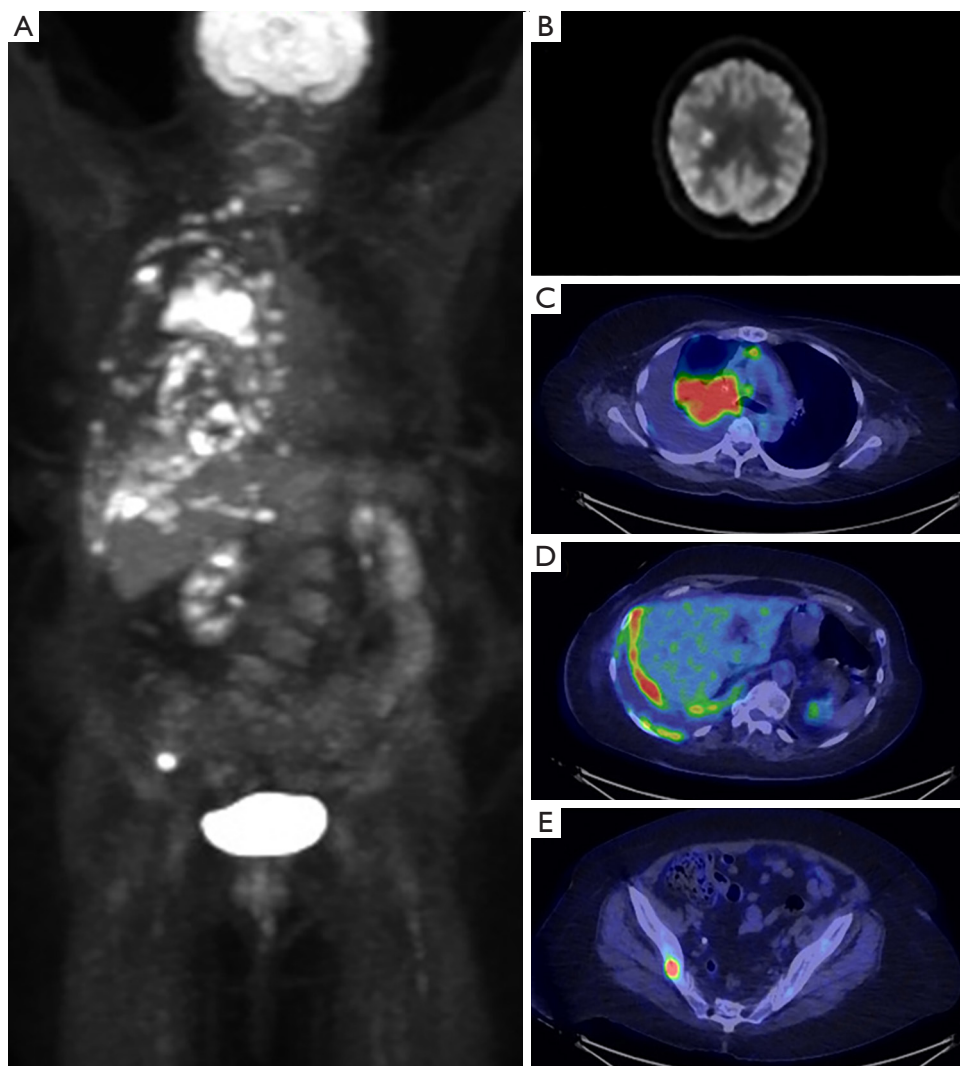


Figure 8 A 73-year-old female presenting for initial staging of NSCL demonstrating the utility of FDG PET/CT. MIP reconstruction (A) demonstrates widespread metastatic disease. Axial fused PET/CT images show: hypermetabolic right brain metastasis (B), hypermetabolic primary right upper lobe malignancy (C), right pleural metastasis (D) and right iliac bone metastasis (E).

positives are more likely in the elderly, diabetics, and were associated with increased interleukin-6 (IL-6) levels, or positive T-spot tuberculosis tests (29).

False negative

False-negative findings at PET can be the result of a small nodule size, low cellular density in lesions or low tumor avidity for FDG. Common false negative histologies included minimal to noninvasive adenocarcinomas (Figure 9), mucinous adenocarcinomas, lymphoma, and carcinoid tumor (15,30,31). The most important radiologic factor for risk assessment is lesion stability versus change

over serial imaging (25). In solitary pulmonary nodules that demonstrate negative findings at PET, serial CT follow-up imaging may be performed in a patient with a low pretest likelihood of malignancy. In a patient with a high pretest likelihood of malignancy, tissue sampling or resection should be considered (32).

SCLC

SCLC has traditionally been staged via the Veterans Administration Lung Study Group (VALSG) 2-stage classification scheme: limited-stage (LS-SCLC) or

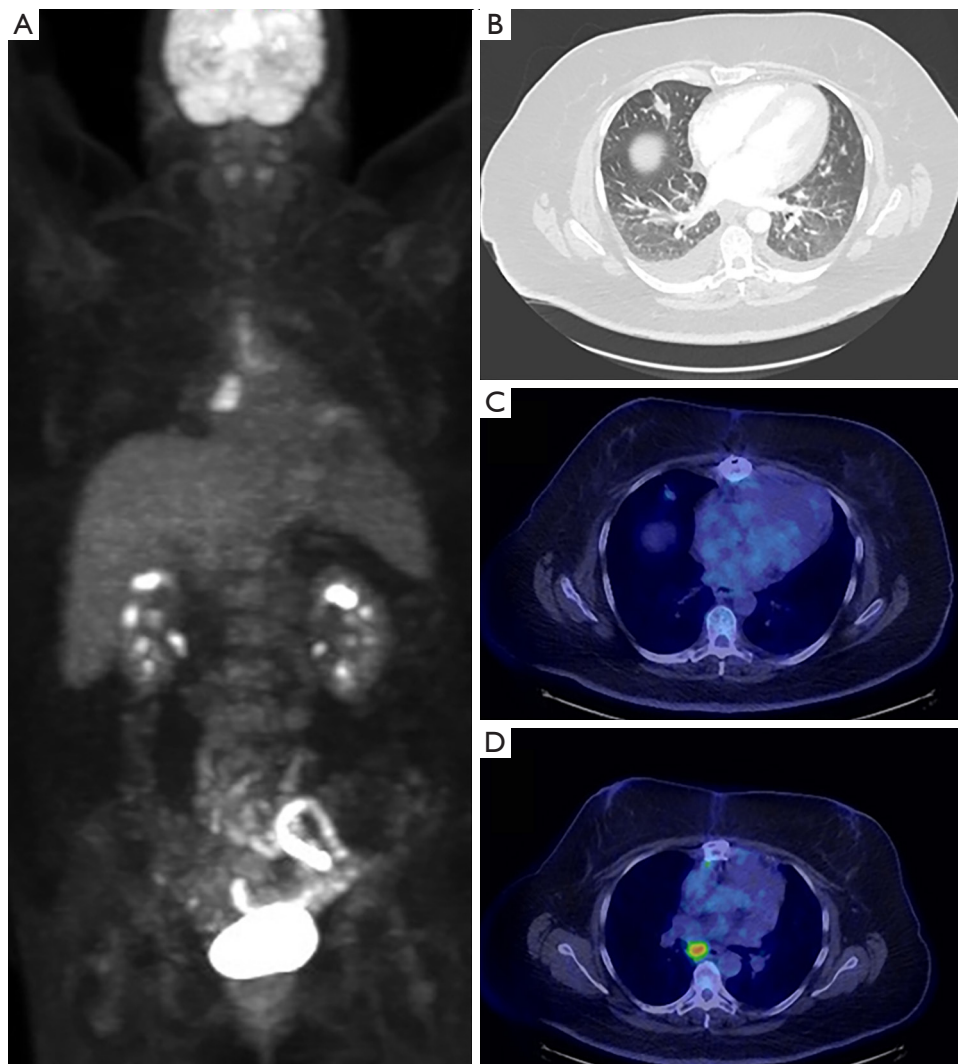


Figure 9 A 58-year-old female with incidentally discovered right middle lobe pulmonary nodule found on a CTA of the chest performed to evaluate for pulmonary embolus. Follow up CT 1 month later showed that the nodule remained, therefore FDG PET/CT was obtained (A). The pulmonary nodule (B) demonstrated low-level FDG uptake (C), and an FDG avid right mediastinal lymph node (D) was also noted. Given relative discrepancy with greater uptake in the lymph node than in the nodule, this was initially favored to represent granulomatous inflammation rather than malignancy, however, biopsy of the lymph node revealed metastatic lung adenocarcinoma.

Extensive-stage (ES-SCLC). Recently, the IASLC proposed that the newly revised TNM staging classification for lung cancer should replace the VALSG system for SCLC (33).

Findings at FDG PET/CT can lead to a change in initial management in up to 27% of patients with SCLC, and a change in overall disease stage in 32% of patients. In addition, the radiation field can be modified in up to 68% of patients due to overall improved characterization of intrathoracic disease (34-37).

Bronchogenic carcinoma prognosis

While PET/CT is a valuable resource in defining bronchogenic carcinoma anatomically with regards to TNM staging, it also holds important prognostic information in a variety of quantifiable PET parameters. SUV max measures only the highest SUV measurement in a single voxel within a region of interest. Studies have shown that SUV max alone does not significantly correlate with survival outcomes, particularly with SCLC (38,39). Additional parameters that can predict lung cancer prognosis include metabolic tumor

volume (MTV) and total lesion glycolysis (TLG). MTV is calculated using a fixed voxel-based SUV threshold and sums all voxels with SUV values greater than or equal to the threshold. TLG is calculated by multiplying MTV by the mean SUV max. Recent studies have found that high MTV and high TLG were associated with a significantly poorer prognosis in NSCLC and SCLC (40,41).

Bronchogenic carcinoma post treatment imaging

After curative treatment of bronchogenic carcinoma, surveillance imaging with CT is recommended every 6 months for 2 years and annually after 2 years by the American Society of Clinical Oncology (42). Despite evidence of high diagnostic performance with improved sensitivity and specificity over CT for recurrence, PET/CT is not recommended (43). Some of the cited reasons include increased cost and radiation exposure of PET/CT (42). However, one recognized application of PET/CT post therapy includes the differentiation of tumor progression or radiation pneumonitis. Radiation pneumonitis may potentially be differentiated from residual or recurrent tumor mainly based off of pattern or FDG uptake. The three patterns of radiation pneumonitis described by Iravani *et al.* include subpleural/patchy, diffuse, and peripheral (34).

¹⁸F-FDG PET/MRI

Despite challenges in MR imaging of the chest due to low proton density and respiratory motion, ¹⁸F-FDG PET/MRI may still play a role in evaluation of a variety of thoracic disease processes (44).

Pulmonary nodules

Current ¹⁸F-FDG PET/MRI techniques are highly sensitive for the detection for FDG-avid solid pulmonary nodules measuring as small as 5 mm (45). New approaches such as ultrashort echo time sequences (UTE) have been proposed to improve detection of smaller pulmonary nodules, but detection of nodules smaller than 5mm remains challenging (46,47).

Bronchogenic carcinoma

MRI provides greater tissue contrast resolution compared to CT, which may improve delineation of chest wall (Figure 10), diaphragm, or mediastinal invasion, which has

implications for T-staging. ¹⁸F-FDG PET/MRI has been proven to have equivalently high diagnostic performance for T and N staging of NSCLC compared to ¹⁸F-FDG PET/CT (35). ¹⁸F-FDG PET/MRI may have greater sensitivity in detecting mediastinal lymph nodes, however, the clinical impact of different staging results has not been fully investigated (36). In terms of M-staging, MRI offers excellent characterization of common metastatic locations such as the adrenal glands, liver, and the brain, which is already a requirement for staging of advanced lung cancer. In this manner, exams can be tailored to combine the ¹⁸F-FDG PET and MRI information in one examination, providing convenience for patients and referring providers.

Neuroendocrine malignancy

Major strides have been made in the imaging of neuroendocrine tumors including bronchial carcinoid due to the development of PET radiotracers targeting somatostatin receptors. While bronchial carcinoid tumors typically have mild to moderate FDG uptake, the density of somatostatin receptors allows for high quality imaging using ⁶⁸Ga DOTATATE as demonstrated in Figure 11 (14). Typically, carcinoid tumors will show low ¹⁸F-FDG avidity and high ⁶⁸Ga DOTATATE avidity, however this is dependent on the degree of differentiation with more poorly differentiated tumors having greater FDG uptake and lower DOTATATE avidity (37).

⁶⁸Ga DOTATATE has been proven to be superior to previous forms of somatostatin receptor imaging, such as ¹¹¹In-pentetreotide (48). Meta-analysis of the sensitivity and specificity of ⁶⁸Ga DOTATE for detecting neuroendocrine tumors including pulmonary carcinoid tumors measures 93% and 91% respectively (49). The utility and superior imaging characteristics of ⁶⁸Ga DOTATATE have led to change in management for up to 36% of patients (48).

One of the most exciting possibilities for neuroendocrine tumors is the role of peptide receptor radionuclide therapy (PRRT) with ¹⁷⁷Lu DOTATATE. ¹⁷⁷Lu DOTATATE contains the same somatostatin receptor analog, DOTATATE, however instead of the ⁶⁸Ga radionuclide used for diagnostic imaging, ¹⁷⁷Lu is incorporated. The therapeutic agent binds to the cell surface somatostatin receptor and then undergoes β -radioactive decay, damaging DNA and resulting in cellular apoptosis. PRRT with ¹⁷⁷Lu DOTATATE for lung carcinoid tumor was not studied under the NETTER-1 trial of gastrointestinal neuroendocrine tumors, however, preliminary evidence

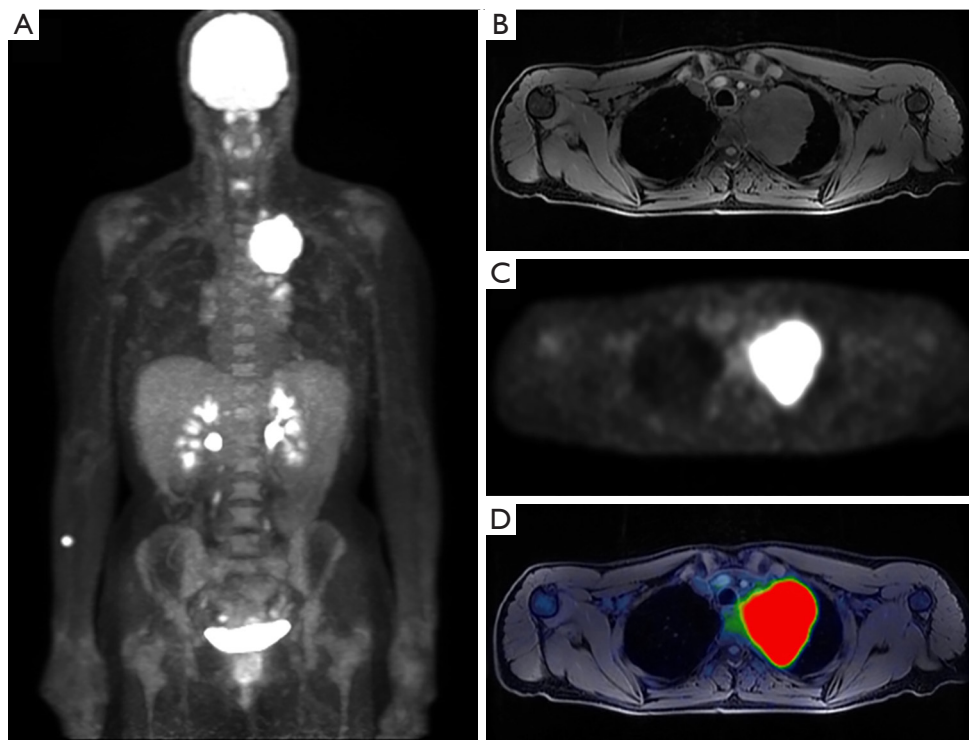


Figure 10 A 44-year-old female presenting with 30 lb weight loss and sharp upper left chest pain found to have a left upper lobes mass on chest radiograph (not shown). Staging FDG PET/MR without IV contrast was performed. MIP reconstruction (A) demonstrates an FDG avid Pancoast tumor with additional FDG avid left cervical and hilar lymph nodes. T1 weighted image with fat saturation (B), axial PET (C) and fused (D) images further delineate degree of mediastinal invasion.

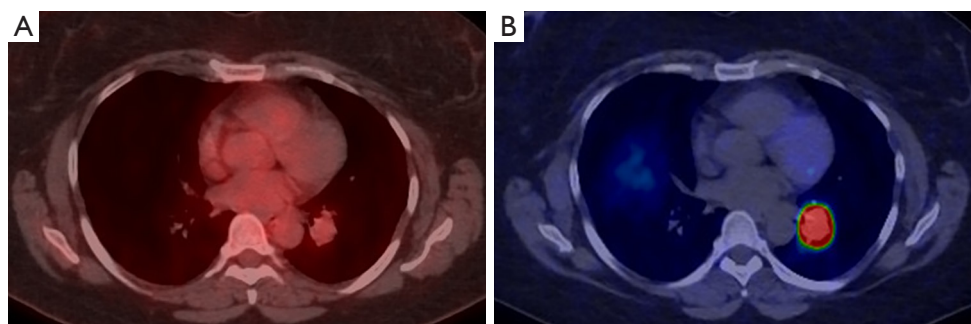


Figure 11 A 56-year-old female found to have a left upper lobe nodule on Chest CT (not shown) performed to evaluate for shortness of breath. Axial fused FDG PET/CT (A) shows a left parahilar nodule with only low-grade uptake (SUVmax 1.7). Subsequently performed axial DOTATATE PET/CT image (B) demonstrates intense radiotracer uptake within the nodule (SUVmax 44.8). Histologic evaluation following surgical resection revealed a typical bronchial type carcinoid tumor.

suggests similar efficacy and safety of PRRT in patients with pulmonary carcinoid tumor (50,51).

Conclusions

Capitalizing on the strength of combining anatomic and physiological imaging, nuclear medicine, and specifically PET, serves a vital role in the evaluation of thoracic disorders, enhancing the care of patients. This invaluable clinical tool includes well-recognized applications such as in evaluation of pulmonary nodules and staging of bronchogenic carcinoma. Emerging technologies have found new roles in PET/MRI and ⁶⁸Ga DOTATATE PET, as well as radionuclide therapy.

Acknowledgments

Funding: None.

Footnote

Provenance and Peer Review: This article was commissioned by the Guest Editor (Chi Wan Koo) for the series “Contemporary Practice in Thoracic Neoplasm Diagnosis, Evaluation and Treatment” published in *Journal of Thoracic Disease*. The article was sent for external peer review organized by the Guest Editor and the editorial office.

Conflicts of Interest: All authors have completed the ICMJE uniform disclosure form (available at: <http://dx.doi.org/10.21037/jtd-2019-cptn-09>). The series “Contemporary Practice in Thoracic Neoplasm Diagnosis, Evaluation and Treatment” was commissioned by the editorial office without any funding or sponsorship. The authors have no other conflicts of interest to declare.

Ethical Statement: The authors are accountable for all aspects of the work in ensuring that questions related to the accuracy or integrity of any part of the work are appropriately investigated and resolved.

Open Access Statement: This is an Open Access article distributed in accordance with the Creative Commons Attribution-NonCommercial-NoDerivs 4.0 International License (CC BY-NC-ND 4.0), which permits the non-commercial replication and distribution of the article with the strict proviso that no changes or edits are made and the original work is properly cited (including links to both the

formal publication through the relevant DOI and the license). See: <https://creativecommons.org/licenses/by-nc-nd/4.0/>.

References

1. Lillington GA. Management of solitary pulmonary nodules. *Disease-a-Month* 1991;37:269-318.
2. Bunyaviroch T, Coleman RE. PET evaluation of lung cancer. *J Nucl Med* 2006;47:451-69.
3. Bury T, Dowlati A, Paulus P, et al. Evaluation of the solitary pulmonary nodule by positron emission tomography imaging. *Eur Respir J* 1996;9:410-4.
4. Higashi K, Matsunari I, Ueda Y, et al. Value of whole-body FDG PET in management of lung cancer. *Ann Nucl Med* 2003;17:1-14.
5. Hochhegger B, Alves GR, Irion KL, et al. PET/CT imaging in lung cancer: indications and findings. *J Bras Pneumol* 2015;41:264-74.
6. Hansell DM, Bankier AA, MacMahon H, et al. Fleischner Society: glossary of terms for thoracic imaging. *Radiology* 2008;246:697-722.
7. Christensen JA, Nathan MA, Mullan BP, et al. Characterization of the solitary pulmonary nodule: 18F-FDG PET versus nodule-enhancement CT. *AJR Am J Roentgenol* 2006;187:1361-7.
8. Behzadi A, Ung Y, Lowe V, et al. The role of positron emission tomography in the management of non-small cell lung cancer. *Can J Surg* 2009;52:235-42.
9. Lowe VJ, Hoffman JM, DeLong DM, et al. Semiquantitative and visual analysis of FDG-PET images in pulmonary abnormalities. *J Nucl Med* 1994;35:1771-6.
10. Cronin P, Dwamena BA, Kelly AM, et al. Solitary pulmonary nodules: meta-analytic comparison of cross-sectional imaging modalities for diagnosis of malignancy. *Radiology* 2008;246:772-82.
11. Daniels CE, Lowe VJ, Aubry MC, et al. The utility of fluorodeoxyglucose positron emission tomography in the evaluation of carcinoid tumors presenting as pulmonary nodules. *Chest* 2007;131:255-60.
12. Nagelschneider AA, Broski SM, Holland WP, et al. The flip-flop fungus sign: an FDG PET/CT sign of benignity. *Am J Nucl Med Mol Imaging* 2017;7:212-7.
13. Johnson GB, Peller PJ, Kemp BJ, et al. Future of thoracic PET scanning. *Chest* 2015;147:25-30.
14. Erasmus JJ, McAdams HP, Patz EF Jr, et al. Evaluation of primary pulmonary carcinoid tumors using FDG PET. *AJR Am J Roentgenol* 1998;170:1369-73.
15. Berger KL, Nicholson SA, Dehdashti F, et al. FDG

- PET evaluation of mucinous neoplasms: correlation of FDG uptake with histopathologic features. *AJR Am J Roentgenol* 2000;174:1005-8.
16. Erasmus JJ, Macapinlac HA. Low-sensitivity FDG-PET studies: less common lung neoplasms. *Semin Nucl Med* 2012;42:255-60.
 17. Chun EJ, Lee HJ, Kang WJ, et al. Differentiation between malignancy and inflammation in pulmonary ground-glass nodules: The feasibility of integrated 18F-FDG PET/CT. *Lung Cancer* 2009;65:180-6.
 18. Ettinger DS, Wood DE, Aisner DL, et al. Non-Small Cell Lung Cancer, Version 5.2017, NCCN Clinical Practice Guidelines in Oncology. *J Natl Compr Canc Netw* 2017;15:504-35.
 19. Silvestri GA, Gonzalez AV, Jantz MA, et al. Methods for staging non-small cell lung cancer: Diagnosis and management of lung cancer, 3rd ed: American College of Chest Physicians evidence-based clinical practice guidelines. *Chest* 2013;143:e211S-e50S.
 20. Ravenel JG, Rosenzweig KE, Kirsch J, et al. ACR Appropriateness Criteria non-invasive clinical staging of bronchogenic carcinoma. *J Am Coll Radiol* 2014;11:849-56.
 21. Takeuchi S, Khiewvan B, Fox PS, et al. Impact of initial PET/CT staging in terms of clinical stage, management plan, and prognosis in 592 patients with non-small-cell lung cancer. *Eur J Nucl Med Mol Imaging* 2014;41:906-14.
 22. Gregory DL, Hicks RJ, Hogg A, et al. Effect of PET/CT on management of patients with non-small cell lung cancer: results of a prospective study with 5-year survival data. *J Nucl Med* 2012;53:1007-15.
 23. Detterbeck FC, Boffa DJ, Kim AW, et al. The Eighth Edition Lung Cancer Stage Classification. *Chest* 2017;151:193-203.
 24. Gould MK, Kuschner WG, Ryzak CE, et al. Test performance of positron emission tomography and computed tomography for mediastinal staging in patients with non-small-cell lung cancer: a meta-analysis. *Ann Intern Med* 2003;139:879-92.
 25. Kubota K, Matsuno S, Morioka N, et al. Impact of FDG-PET findings on decisions regarding patient management strategies: a multicenter trial in patients with lung cancer and other types of cancer. *Ann Nucl Med* 2015;29:431-41.
 26. Li J, Xu W, Kong F, et al. Meta-analysis: accuracy of 18FDG PET-CT for distant metastasis staging in lung cancer patients. *Surg Oncol* 2013;22:151-5.
 27. Bury T, Barreto A, Daenen F, et al. Fluorine-18 deoxyglucose positron emission tomography for the detection of bone metastases in patients with non-small cell lung cancer. *Eur J Nucl Med* 1998;25:1244-7.
 28. Kumar R, Xiu Y, Yu JQ, et al. 18F-FDG PET in evaluation of adrenal lesions in patients with lung cancer. *J Nucl Med* 2004;45:2058-62.
 29. Feng M, Yang X, Ma Q, et al. Retrospective analysis for the false positive diagnosis of PET-CT scan in lung cancer patients. *Medicine* 2017;96:e7415.
 30. Kuriyama K, Seto M, Kasugai T, et al. Ground-glass opacity on thin-section CT: value in differentiating subtypes of adenocarcinoma of the lung. *AJR Am J Roentgenol* 1999;173:465-9.
 31. Koss MN, Hochholzer L, Nichols PW, et al. Primary non-Hodgkin's lymphoma and pseudolymphoma of lung: a study of 161 patients. *Hum Pathol* 1983;14:1024-38.
 32. Gould MK, Donington J, Lynch WR, et al. Evaluation of individuals with pulmonary nodules: when is it lung cancer? Diagnosis and management of lung cancer, 3rd ed: American College of Chest Physicians evidence-based clinical practice guidelines. *Chest* 2013;143:e93S-e120S.
 33. Kalemkerian GP, Gadgeel SM. Modern staging of small cell lung cancer. *J Natl Compr Canc Netw* 2013;11:99-104.
 34. Iravani A, Turgeon G-A, Akhurst T, et al. PET-detected pneumonitis following curative-intent chemoradiation in non-small cell lung cancer (NSCLC): recognizing patterns and assessing the impact on the predictive ability of FDG-PET/CT response assessment. *Eur J Nucl Med Mol Imaging* 2019;46:1869-77.
 35. Kirchner J, Sawicki LM, Nensa F, et al. Prospective comparison of (18)F-FDG PET/MRI and (18)F-FDG PET/CT for thoracic staging of non-small cell lung cancer. *Eur J Nucl Med Mol Imaging* 2019;46:437-45.
 36. Schaarschmidt BM, Grueneisen J, Metzenmacher M, et al. Thoracic staging with (18)F-FDG PET/MR in non-small cell lung cancer - does it change therapeutic decisions in comparison to (18)F-FDG PET/CT? *Eur Radiol* 2017;27:681-8.
 37. Kayani I, Bomanji JB, Groves A, et al. Functional imaging of neuroendocrine tumors with combined PET/CT using 68Ga-DOTATATE (DOTA-DPhe1, Tyr3-octreotate) and 18F-FDG. *Cancer* 2008;112:2447-55.
 38. Cuccurullo V, Mansi L. *AJCC cancer staging handbook: From the AJCC cancer staging manual*. Springer, 2011.
 39. Ettinger DS, Wood DE, Akerley W, et al. Non-small cell lung cancer, version 1.2015. *J Natl Compr Canc Netw* 2014;12:1738-61.

40. Chen HH, Chiu NT, Su WC, et al. Prognostic value of whole-body total lesion glycolysis at pretreatment FDG PET/CT in non-small cell lung cancer. *Radiology* 2012;264:559-66.
41. Liao S, Penney BC, Wroblewski K, et al. Prognostic value of metabolic tumor burden on 18F-FDG PET in nonsurgical patients with non-small cell lung cancer. *Eur J Nucl Med Mol Imaging* 2012;39:27-38.
42. Schneider BJ, Ismaila N, Aerts J, et al. Lung Cancer Surveillance After Definitive Curative-Intent Therapy: ASCO Guideline. *J Clin Oncol* 2020;38:753-66.
43. Antoniou AJ, Marcus C, Tahari AK, et al. Follow-up or Surveillance (18)F-FDG PET/CT and Survival Outcome in Lung Cancer Patients. *J Nucl Med* 2014;55:1062-8.
44. Ehman EC, Johnson GB, Villanueva-Meyer JE, et al. PET/MRI: Where might it replace PET/CT? *J Magn Reson Imaging* 2017;46:1247-62.
45. Chandarana H, Heacock L, Rakheja R, et al. Pulmonary nodules in patients with primary malignancy: comparison of hybrid PET/MR and PET/CT imaging. *Radiology* 2013;268:874-81.
46. Burris NS, Johnson KM, Larson PE, et al. Detection of Small Pulmonary Nodules with Ultrashort Echo Time Sequences in Oncology Patients by Using a PET/MR System. *Radiology* 2016;278:239-46.
47. Crimi F, Varotto A, Orsatti G, et al. Lung visualisation on PET/MRI: implementing a protocol with a short echo-time and low flip-angle volumetric interpolated breath-hold examination sequence. *Clin Radiol* 2020;75:239.e15-e21.
48. Deppen SA, Liu E, Blume JD, et al. Safety and efficacy of 68Ga-DOTATATE PET/CT for diagnosis, staging, and treatment management of neuroendocrine tumors. *J Nucl Med* 2016;57:708-14.
49. Treglia G, Castaldi P, Rindi G, et al. Diagnostic performance of Gallium-68 somatostatin receptor PET and PET/CT in patients with thoracic and gastroenteropancreatic neuroendocrine tumours: a meta-analysis. Springer, 2012.
50. Strosberg J, Wolin E, Chasen B, et al. 6LBA 177-Lu-Dotatate significantly improves progression-free survival in patients with midgut neuroendocrine tumours: results of the phase III NETTER-1 trial. *Eur J Cancer* 2015;51:S710.
51. Naraev BG, Ramirez RA, Kendi AT, et al. Peptide Receptor Radionuclide Therapy for Patients With Advanced Lung Carcinoids. *Clin Lung Cancer* 2019;20:e376-92.

Cite this article as: Jaykel TJ, Clark MS, Adamo DA, Welch BT, Thompson SM, Young JR, Ehman EC. Thoracic positron emission tomography: ¹⁸F-fluorodeoxyglucose and beyond. *J Thorac Dis* 2020;12(11):6978-6991. doi: 10.21037/jtd-2019-cptn-09